Inscopix: miniature microscope for circuit neuroscience

Eleanna Kara

Technical journal club

5/2/2019

In vivo calcium imaging is crucial for understanding circuit function and dysfunction

Conventional methods:

- Tabletop optical instrumentation that cannot be readily distributed to many mice in parallel
- Head fixation of the mouse - incompatible with standard rodent behavioral assays

Inscopix nVista:

- In vivo calcium imaging in awake, behaving mice through miniature microscopes attached to the mouse's head

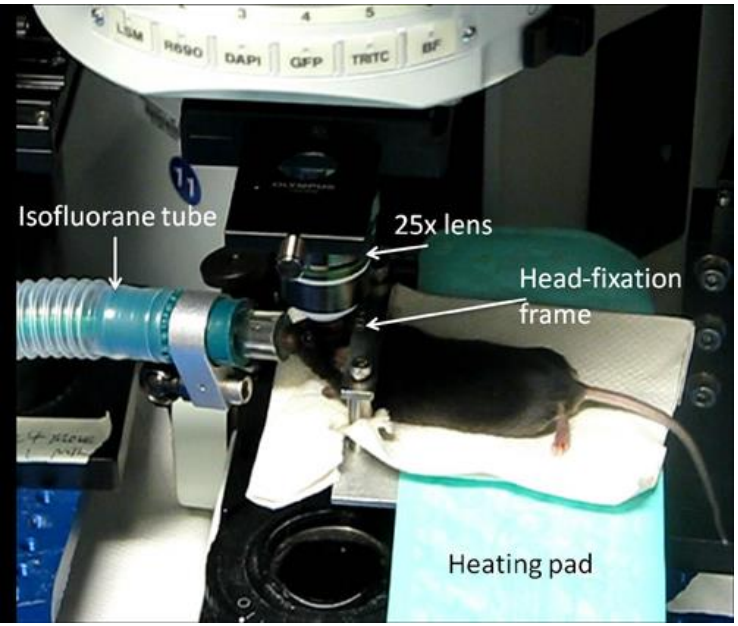

Cao et al, 2013 Jove

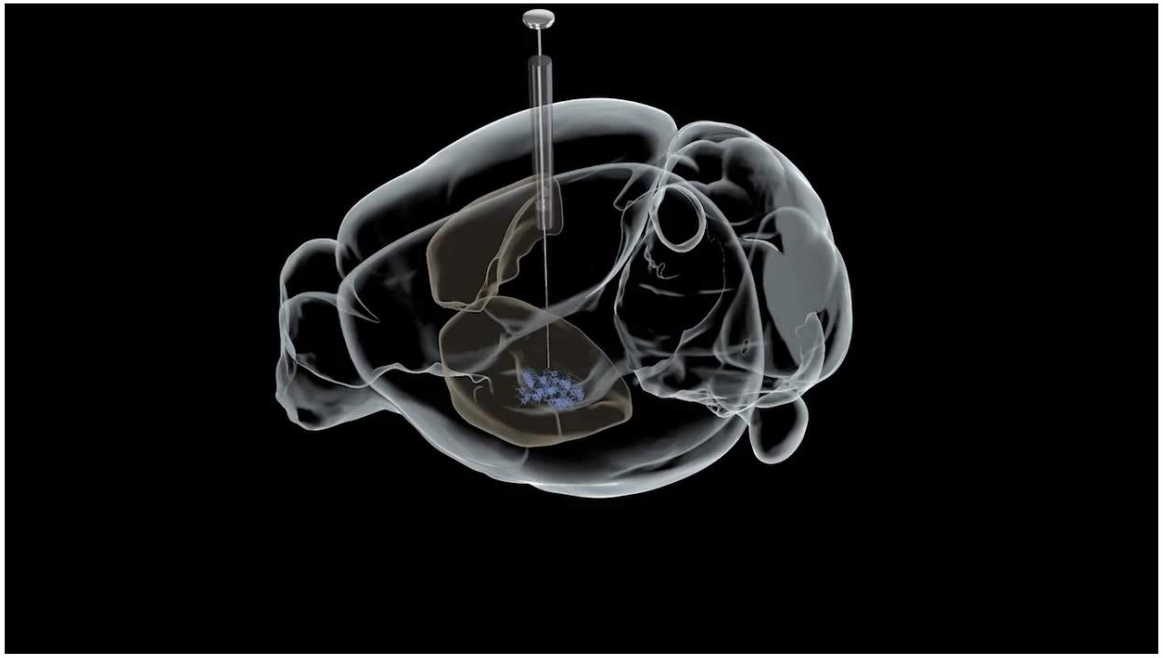

Video from inscopix website

Miniaturized integration of a fluorescence microscope

Kunal K Ghosh[1,2,5], Laurie D Burns[2,5], Eric D Cocker[2,5], Axel Nimmerjahn[2], Yaniv Ziv[2], Abbas El Gamal[1] & Mark J Schnitzer[2–4]

- 2011

- 1,9gr
  - Portable by adult mouse

- Doesn't restrict movement
  - Fiber optics microscopes exert torque on mouse

- 500% increase in optical throughput compared to fiber optics microscope (2008)
- Improvement in data quality

  - Capillaries
  - Ca2+ spikes
  - Larger numbers of neurons (700% increase)

- Hardware improvements:
  - Lower illumination
  - 1h imaging sessions
  - Lower photobleaching

Design of inscopix microscope

Recent advances in optoelectronics have yielded inexpensive but high-quality parts

- Tiny but bright light-emitting diodes (LEDs)
- Complementary metal-oxide semiconductor (CMOS) image sensors with fine pixel sizes and high sensitivity
- Incorporation of all optical parts in a ~2.4 cm3 housing

Pathways:
Blue: illumination
Green: emission

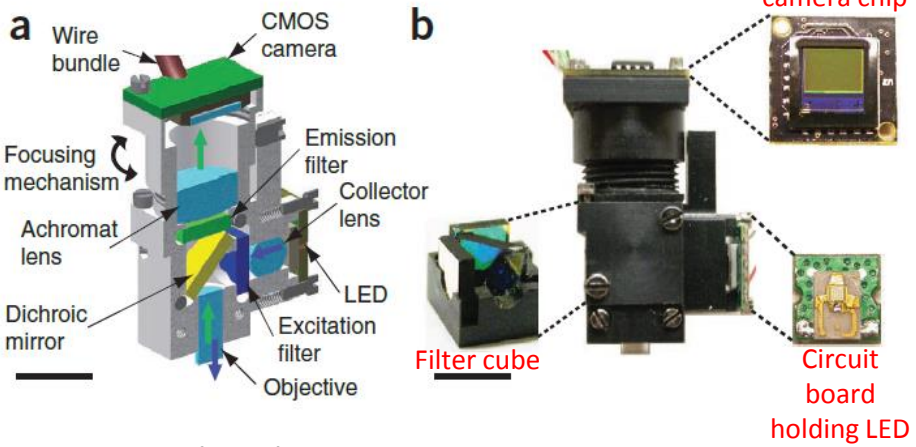

Beam path

- Excitation
  - Blue LED on a custom 6 mm × 6 mm printed circuit board (PCB)
  - Drum lens collects the LED's emissions
  - 4 mm × 4 mm excitation filter
  - dichroic mirror
  - imaging pathway
  - gradient refractive index (GRIN) objective lens
- Emission
  - objective, dichroic, emission filter, achromatic doublet lens, CMOS sensor mounted on a custom 8.4 mm × 8.4 mm PCB

Housing

- Polyetheretherketone
- Focusing to sub-micrometer accuracy by adjusting the camera position

Technical specifications

- Maximum field of view 600 µm × 800 µm
- Optical magnification ~5.0×

Table 1 | Comparison of integrated and fiber bundle–based fluorescence microscopes

	Integrated microscope	Fiber-bundle microscope[6]
Nyquist detection resolution	~2.5 μm	~2.8–3.9 μm
Optical resolution	~1.5 μm	~2.8–3.9 μm
Detection-limited field of view	0.48 mm^2	0.07 mm^2
Optical field of view	1 mm^2	0.07 mm^2
Fluorescence throughput to sensor	~95%	~20%
Signal transmission	Digital image data	Fluorescence photons
Mechanical tether to mouse	Floppy	Deflection-dependent stress
Reference frame of optics	All optics move with mouse	Lamp and camera stay in lab frame
Illumination field at specimen	Does not rotate	Rotates with animal movement
Portability of optics	Fit in wallet or purse	Benchtop instrument on air table
Total system portability	Briefcase-compatible	Benchtop instrument on air table
Portability of optical function	No realignment needed	Optical realignment needed
Cost of optoelectronic parts	~$1–10	~$25,000–50,000
Manufacturing scalability	Mass-producible	No batch fabrication for lamp and camera

Fluorescence throughput is defined here as the efficiency with which captured fluorescence emissions are relayed from the specimen plane to the detection plane. Given the comparable numerical apertures (~0.5) and sensor quantum efficiencies, the fivefold difference in fluorescence throughput is the chief reason the integrated microscope has far greater sensitivity.

Cerebellar microcirculatory dynamics in freely behaving mice

Microvasculature in cerebellar cortex of a freely behaving mouse, after intravascular injection of fluorescein-dextran dye

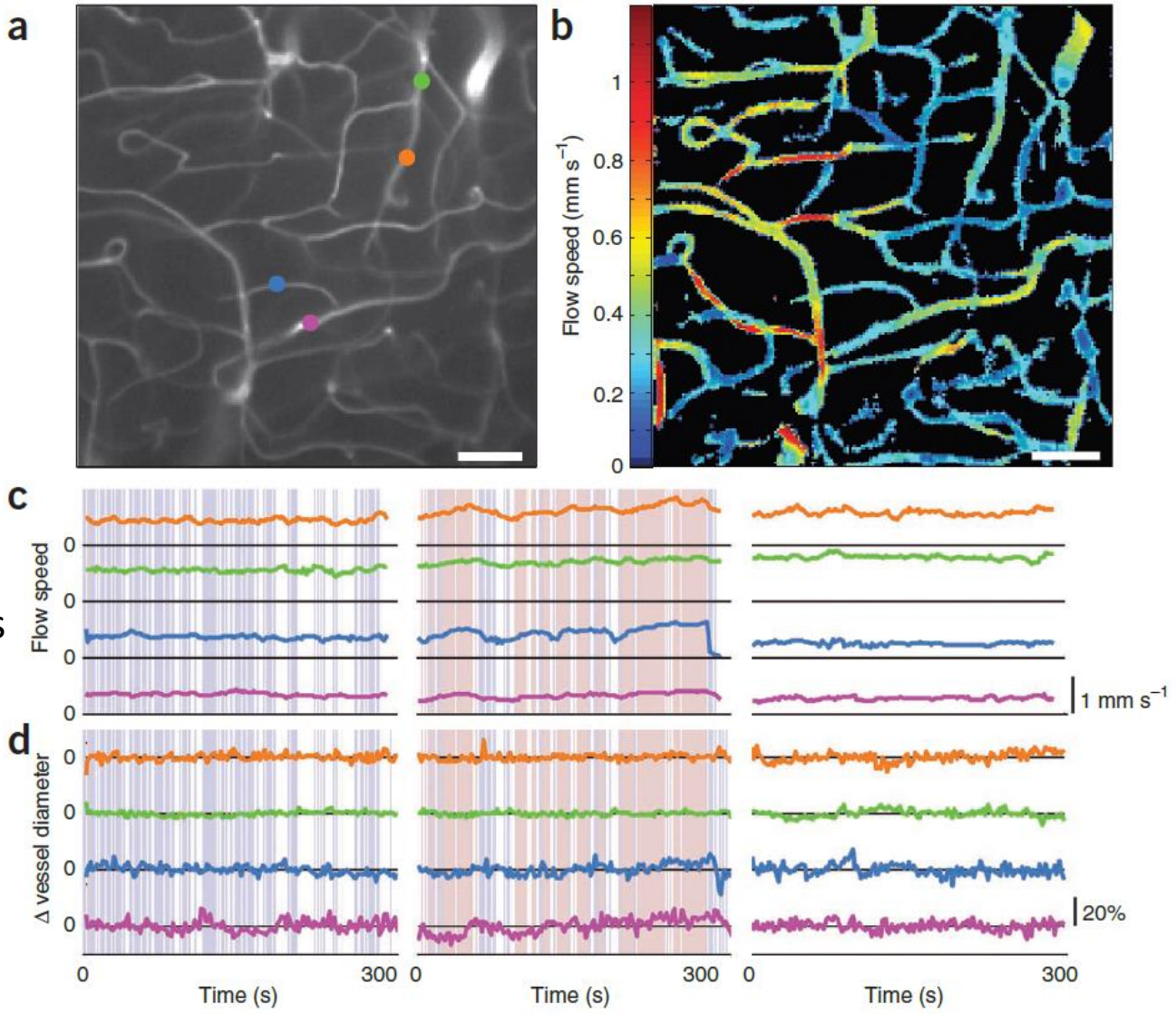

Erythrocyte flow speeds

Vessel diameter changes

- Blue: movement in cage
- Red: running on exercise wheel
- White: rest

Ca2+ spiking in cerebellum

Cerebellar microzones exhibit large-scale, synchronized Ca2+ spiking during motor behavior

Microzone rasters (colored circles)

- Ca2+ spiking
  - >35% (open circles) or
  - >50% (closed circles) of neurons identified in each microzone

Ca2+ spike (black dots) raster plots

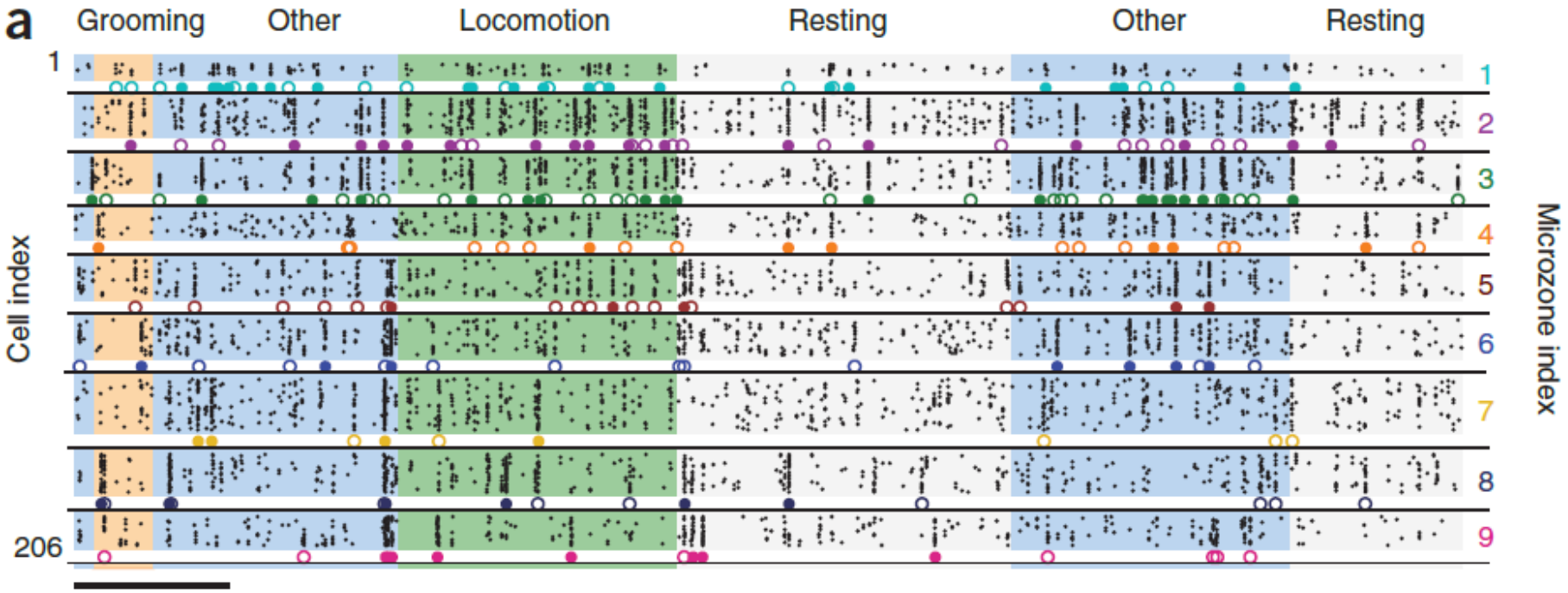

jove Journal of Visualized Experiments www.jove.com

Video Article

Multi-layer Cortical Ca^{2+} Imaging in Freely Moving Mice with Prism Probes and Miniaturized Fluorescence Microscopy

Srishti Gulati[1], Vania Y. Cao[1], Stephani Otte[1]

[1]Inscopix Inc.

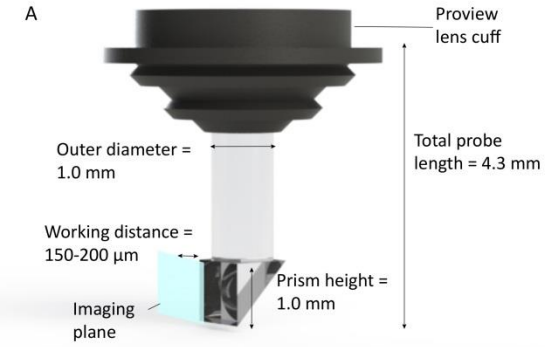
A
Proview
lens cuff
Total probe
length = 4.3 mm
Outer diameter =
1.0 mm
Working distance =
150-200 µm
Prism height =
1.0 mm
Imaging
plane

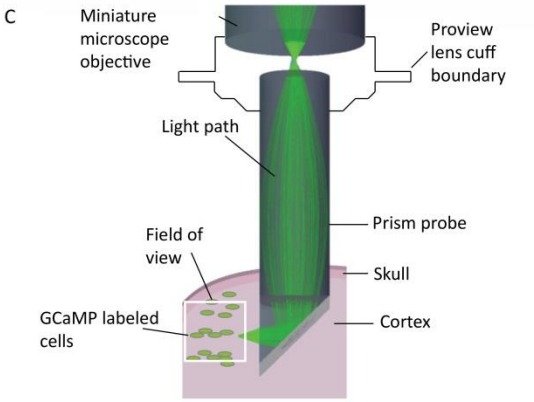
C
Miniature
microscope
objective
Proview
lens cuff
boundary
Light path
Prism probe
Field of
view
Skull
GCaMP labeled
cells
Cortex

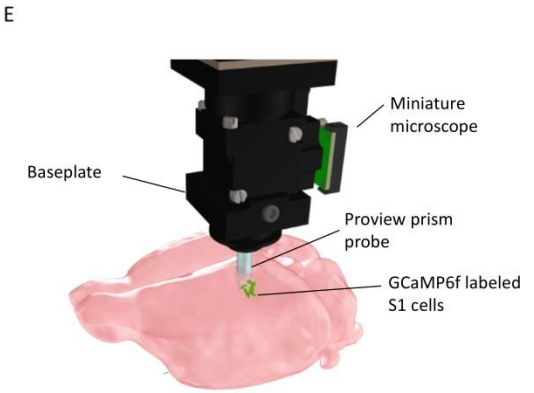
E
Miniature
microscope
Baseplate
Proview prism
probe
GCaMP6f labeled
S1 cells


jove

Postmortem Histological Validation of Prism Probe Location and GCaMP Expression

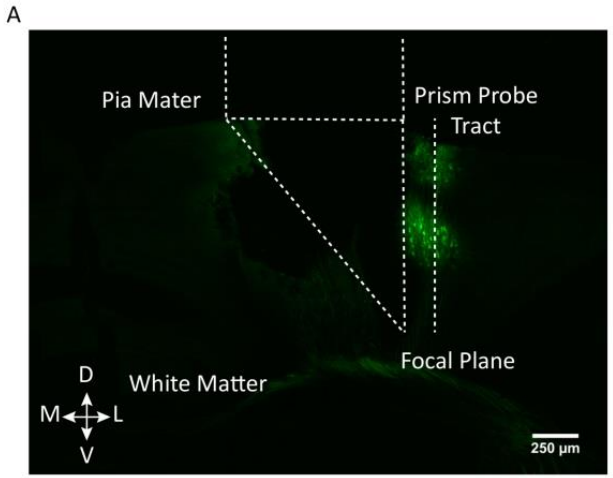

Coronal section from a representative mouse brain showing the prism probe tract and with its imaging side facing the GCaMP6f expressing cells (AAV1.CaMKII.GCaMP6f expressed in neurons in layers 2/3 and 5).

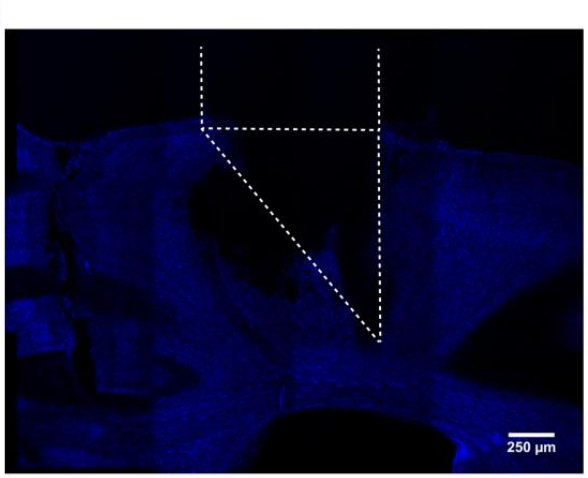

Same coronal brain section following staining for DAPI.

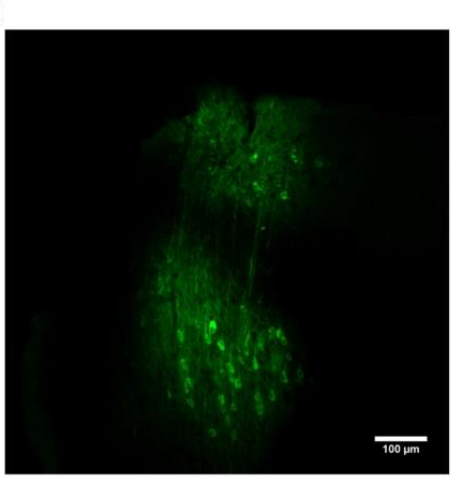

Zoomed in view of GCaMP6f expressing cells in somatosensory cortex.

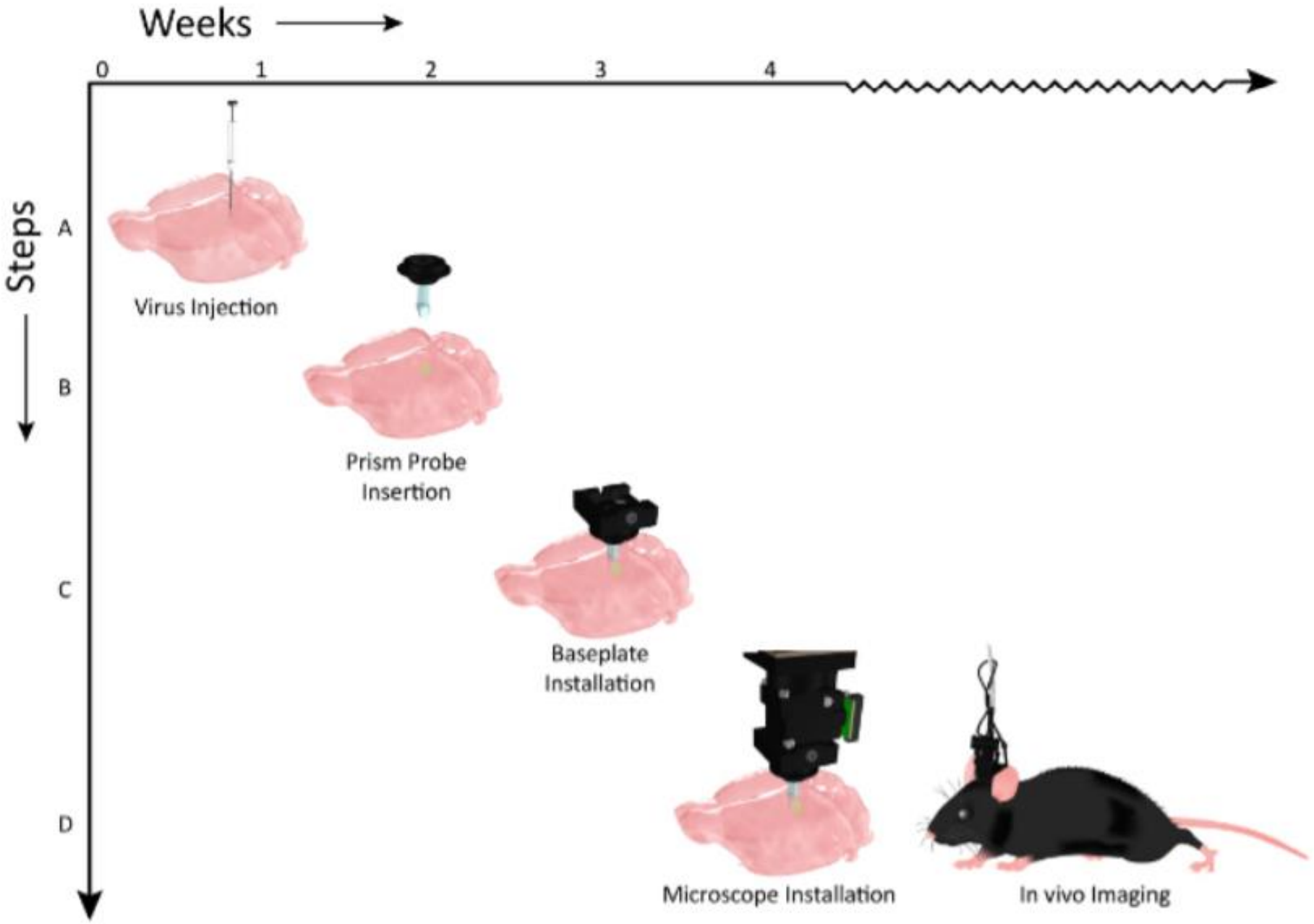
Weeks
0
1
2
3
4
Steps
A
B
C
D
Virus Injection
Prism Probe Insertion
Baseplate Installation
Microscope Installation
In vivo Imaging

A Open Field

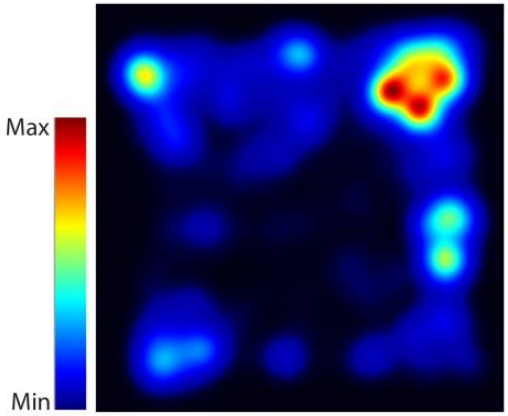

Day 1

B Object Familiarization

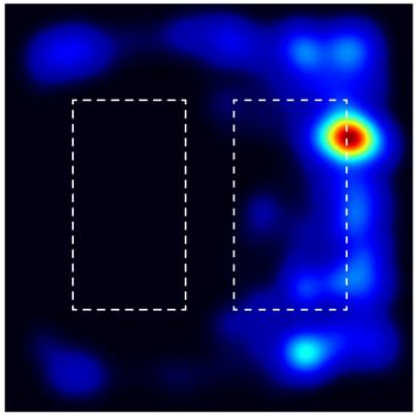

Day 2-4

C Novel Object Exposure

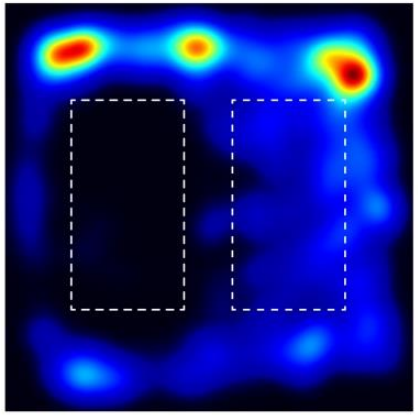

Day 5

Calcium Dynamics from Superficial and Deep Layers of Somatosensory Cortex of a Representative Mouse Imaged with the Microscope

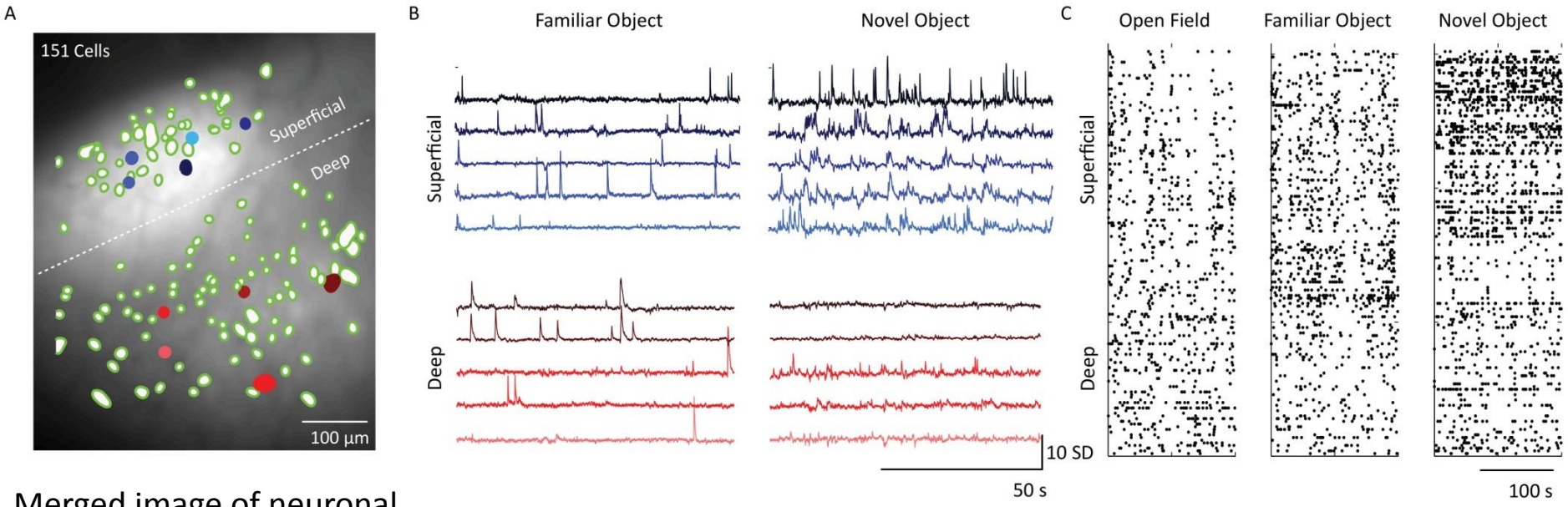

Merged image of neuronal spatial filters (green blobs) and mean fluorescence intensity projection of the microscope recording through prism probe field of view. Border between supragranular and infragranular layers indicated by a white dashed line.

Calcium traces from five example superficial and deep layer cells (filled blue and red cells in panel A)

Layer 2/3 cells were more active compared to layer 5 cells on the day when the mouse was exposed to a novel object.

Inscopix nVoke: combination of calcium imaging and optogenetics

nVoke integrates two LED light sources for simultaneous or sequential cellular resolution imaging using GCaMP indicators and red-shifted opsins for temporally precise control of cells within the same field of view.

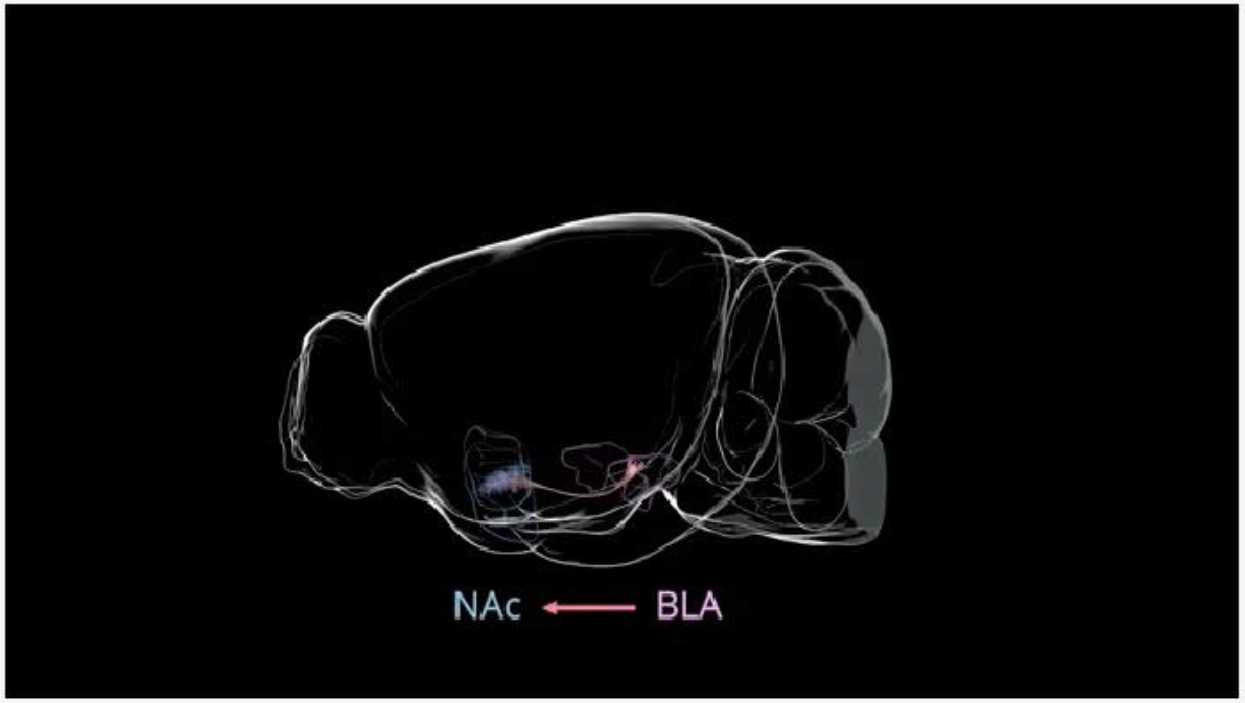

Video from inscopix website

	SAME CELLS[1]	TWO POPULATIONS[1]	TWO POPULATIONS[2]
			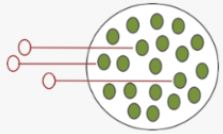
Ca^{2+} IMAGING + OPTOEXCITATION*	UNDER VALIDATION	UNDER VALIDATION	✓ VALIDATED GCaMP6 + ChrimsonR
Ca^{2+} IMAGING + OPTOINHIBITION*	✓ VALIDATED GCaMP6 + NpHR3.0/Jaws	✓ VALIDATED GCaMP6 + NpHR3.0/Jaws	✓ VALIDATED GCaMP6 + NpHR3.0/Jaws

Calcium Indicator (GCaMP6) ○ Opsin (ChrimsonR, NpHR3.0, Jaws) *Sequential & Simultaneous [1]Somal Optogenetics [2]Terminal Optogenetics

LETTER

https://doi.org/10.1038/s41586-018-0682-1

Dopamine enhances signal–to–noise ratio in cortical–brainstem encoding of aversive stimuli

Caitlin M. Vander Weele[1,4], Cody A. Siciliano[1,4], Gillian A. Matthews[1,4], Praneeth Namburi[1], Ehsan M. Izadmehr[1], Isabella C. Espinel[1], Edward H. Nieh[1], Evelien H. S. Schut[1,2], Nancy Padilla–Coreano[1], Anthony Burgos–Robles[1], Chia–Jung Chang[1], Eyal Y. Kimchi[1], Anna Beyeler[1], Romy Wichmann[1,3], Craig P. Wildes[1] & Kay M. Tye[1,3]*

How dopamine released from the ventral tegmental area (VTA) increases the signal-to-noise ratio in the neural circuit from the medial prefrontal cortex (mPFC) to the periaqueductal gray (dPAG) to specifically affect processing of aversive behaviours.

- **nVista:** monitor activity in projection specific populations in the mPFC to observe the activity of mPFC neurons that project to the dPAG compared to those that project to the nucleus accumbens (NAc)

- **nVoke:** combine imaging of mPFC neurons with simultaneous optogenetic stimulation of VTA terminals to show the signal-to-noise ratio is greatly enhanced for aversive stimuli in the mPFC-dPAG circuit, but not the mPFC- NAc circuit.

Background

- Dopamine modulates medial prefrontal cortex (mPFC) activity to mediate diverse behavioural functions; however, the precise circuit computations remain unknown.

- One potentially unifying model by which dopamine may underlie a diversity of functions is by **modulating the signal-to-noise ratio** in subpopulations of mPFC neurons, where neural activity conveying sensory information (signal) is amplified relative to spontaneous firing (noise).

- As mPFC neurons respond to both rewarding and aversive stimuli, and dopamine neurons in the ventral tegmental area (VTA) that project to the mPFC (VTADA–mPFC neurons) are uniquely sensitive to aversive stimuli, the authors proposed that mPFC neurons encoding aversive or rewarding events are differentially modulated by dopamine.

- The authors show that dopamine increases the signal-to-noise ratio of responses to aversive stimuli in mPFC neurons projecting to the dorsal periaqueductal grey (dPAG).

Tail pinch evokes rapid dopamine release in the mPFC and dopamine biases behaviour towards aversion during stimulus competition.

- Fast-scan cyclic voltammetry (FSCV): direct measurement of catecholamine neurotransmission with precise temporal resolution.
- Investigation of the precise time course of dopamine release using FSCV combined with optical and pharmacological approaches to dissect contributions of VTADA neurons.
- Electrodes were aimed at deep layers (5–6) of the mPFC, where VTADA terminals were densest, relative to locus coeruleus (LC) noradrenaline terminals (LCNA)
- Tyrosine hydroxylase (TH)::Cre rats, which expressed halorhodopsin (NpHR) in a Cre-dependent manner in VTADA neurons
- Tail pinches with and without **photoinhibition of VTADA neurons**.
- Photoinhibition of VTADA neurons attenuated the pinch-induced signals in the mPFC.
- VTADA–mPFC neurons contributed the bulk of the rapid pinch-evoked catecholaminergic signal.

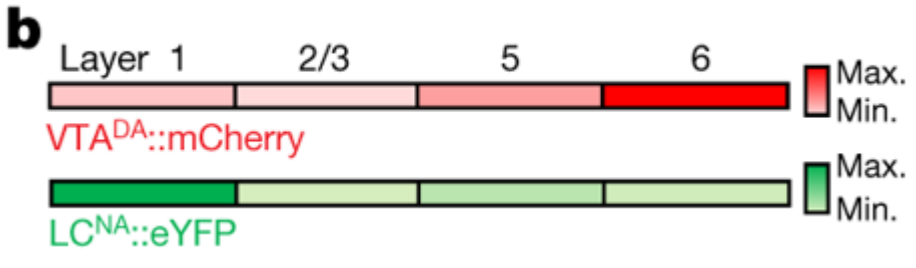

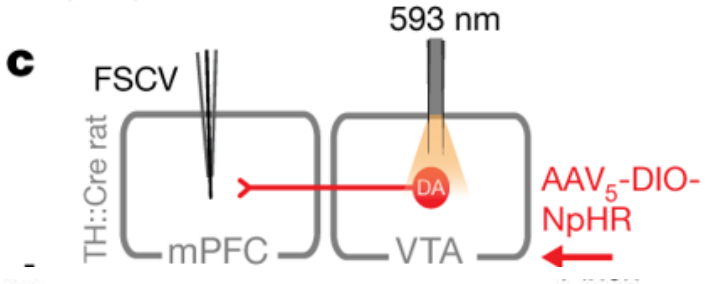

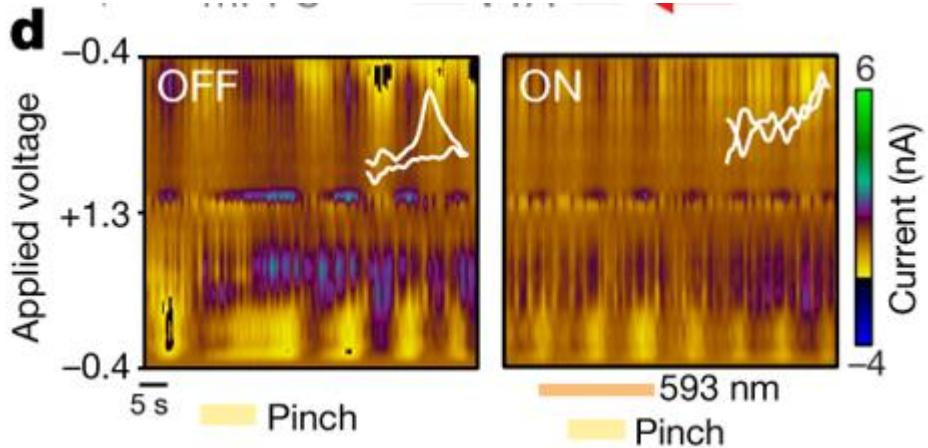

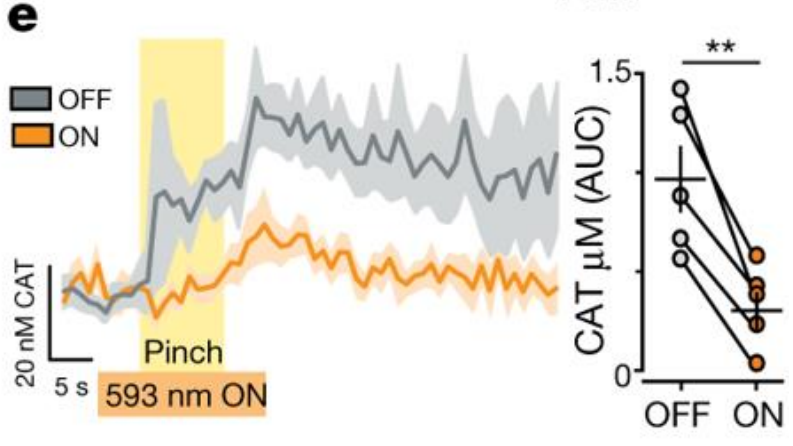

Activation of VTADA terminals in the mPFC does not support real-time or conditioned place preference.

- Explored the causal relationship between VTADA–mPFC and valence processing by testing whether this circuit component was sufficient to promote aversion.
- Reverse experiment: TH::Cre rats to express channelrhodopsin-2 (ChR2) in VTADA neurons, and implanted optical fibres over the mPFC .
- **Activation of VTADA–mPFC terminals** had no effect on behaviour in real-time place avoidance (RTPA) or conditioned place aversion (CPA) assays.

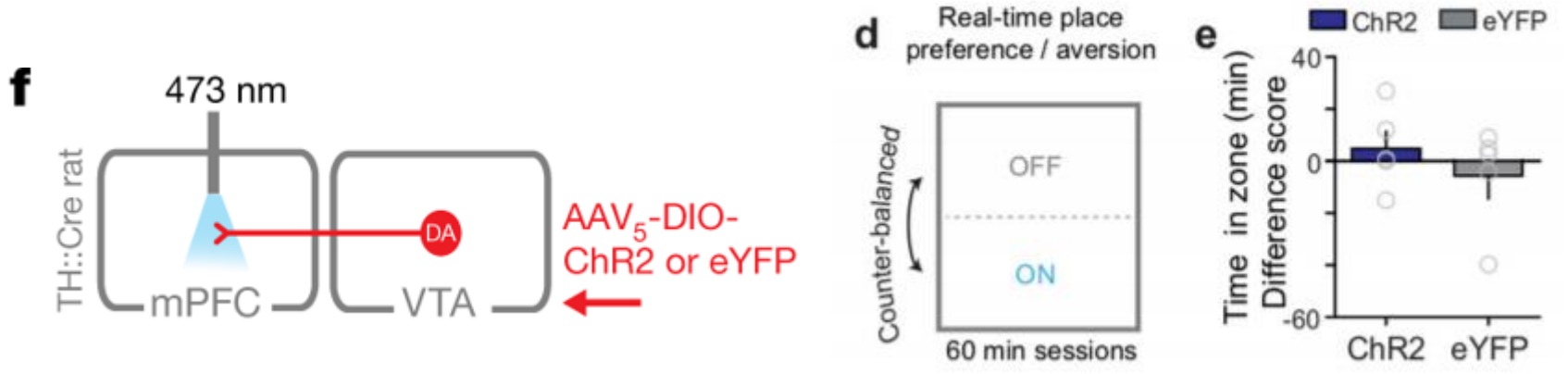

Dopamine enhances responses to discrete, predictive cues

- Trained rats to associate auditory or visual cues (counterbalanced) with either shock or sucrose delivery.

- Tested their behavioural responses to the ‘competition’ of simultaneously presented cues driving conflicting motivational outputs.

- Photostimulation of VTADA–mPFC during the competition trials caused rats expressing ChR2 to spend significantly less time in the sucrose delivery port and more time freezing compared to controls expressing eYFP.

- Conclusion: dopamine is released in a time-locked manner upon presentation of an aversive stimulus, and that VTADA in the mPFC biases behavioural responses towards aversion in the face of conflicting motivational drives.

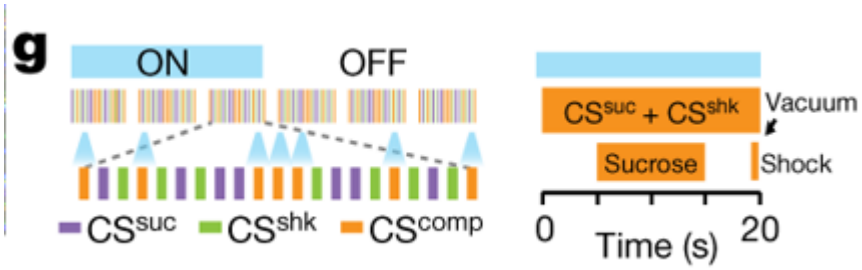

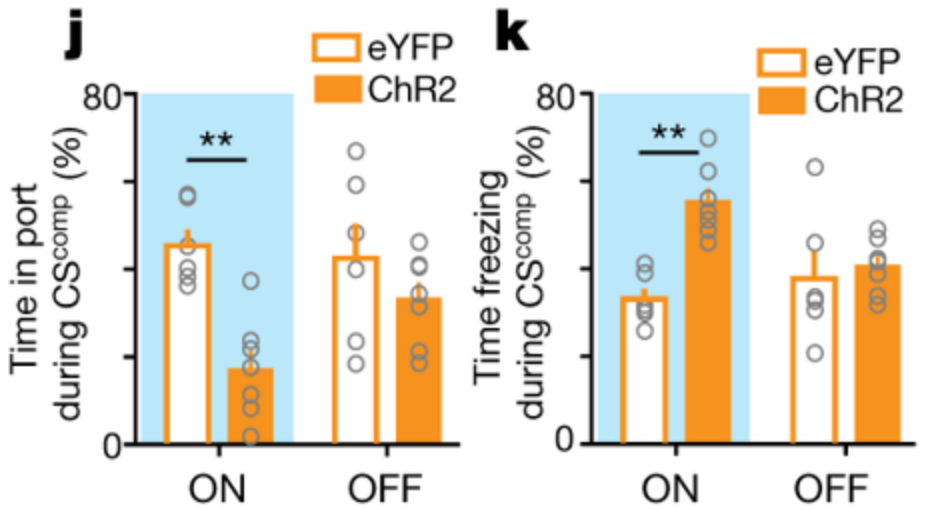

The mPFC promotes aversion through projections to the dPAG

- Identification of distinct, anatomically defined subpopulations in the mPFC that might relay information relevant to processing of aversive information.

- The mPFC has many downstream projection targets, including the periaqueductal grey (PAG) and nucleus accumbens (NAc).

- The mPFC–dPAG circuit and mPFC–NAc projections formed anatomically distinct subpopulations.

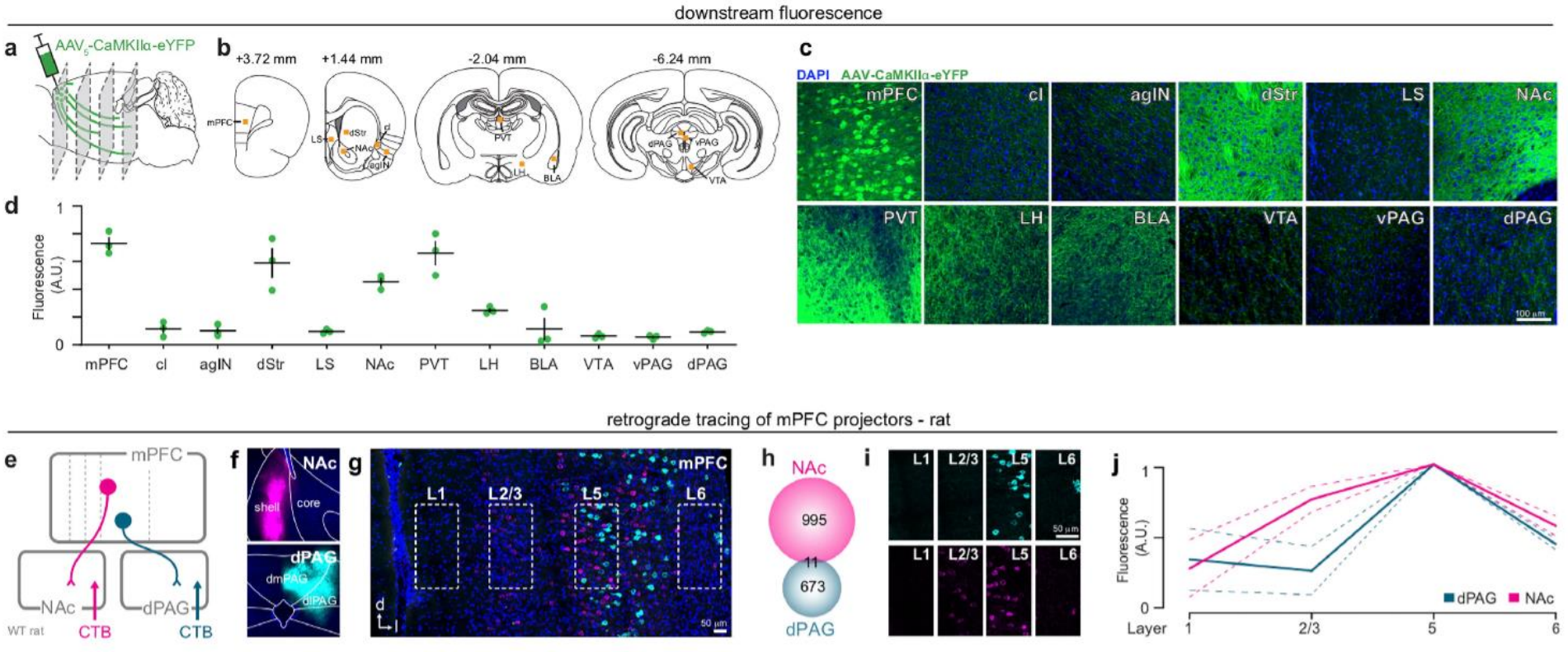

The mPFC promotes aversion through projections to the dPAG.

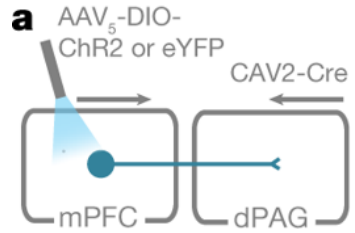

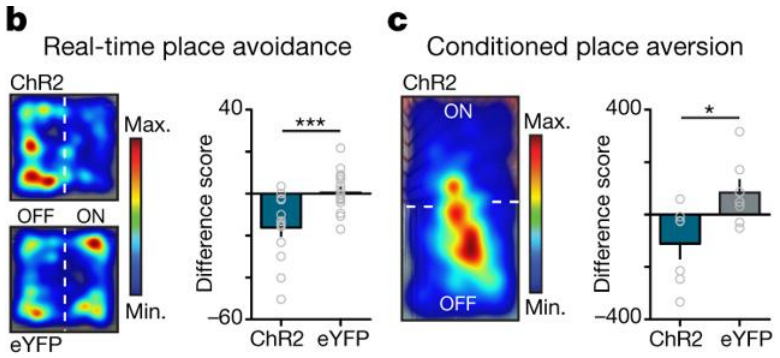

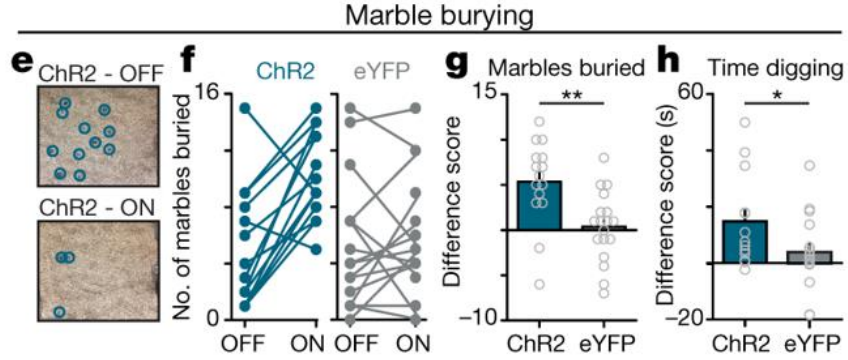

- To target these pathways, ChR2 or eYFP alone was expressed in either mPFC–dPAG or mPFC–NAc neurons.
- Photostimulation of mPFC–NAc neurons did not produce detectable differences in behaviour between ChR2 and eYFP-expressing groups during RTPA or CPA.
- By contrast, activation of ChR2 in mPFC–dPAG neurons reduced the time spent in the light-paired chamber in both RTPA and CPA , relative to eYFP controls.
- Strikingly, photostimulation of mPFC–dPAG produced an increase in marble burying and time spent digging.
- Reverse experiment: The effects in the RTPA and marble-burying assays observed upon activation of mPFC–dPAG somata were reproduced by activation of mPFC terminals directly in the dPAG.

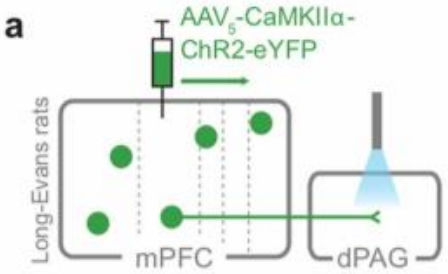

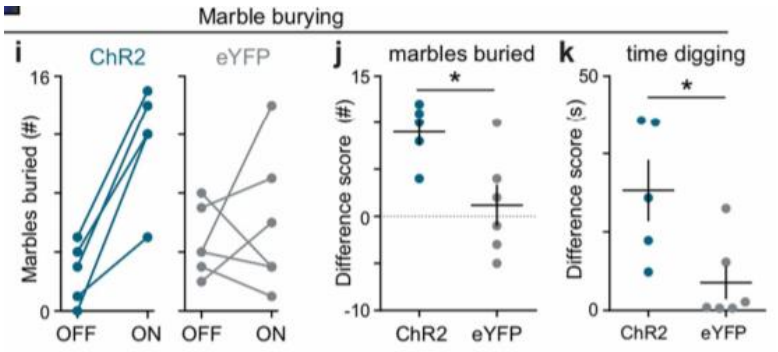

Using inscopix nVista to investigate the dynamics of the mPFC–dPAG and mPFC–NAc populations at the single cell level

- Investigated the dynamics of individual neurons in the mPFC–dPAG and mPFC–NAc populations during shock or sucrose presentation.

- To visualize changes in intracellular calcium concentration indicative of neural activity, the authors selectively expressed GCaMP6m in mPFC–dPAG and mPFC–NAc neurons.

- Assessment of bulk fluorescence activity, a measure of population activity, revealed that the mPFC–NAc population was not significantly modulated by either shock or sucrose.
- By contrast, mPFC–dPAG neurons showed a robust, time-locked increase in activity in response to shock and a decrease in response to sucrose.

- Identified 169 mPFC–NAc and 118 mPFC–dPAG neurons, which sorted into 6 functional clusters. When comparing the normalized responses of individual cells within each population, mPFC–NAc responses were heterogeneous while mPFC–dPAG responses were robustly biased towards shock.

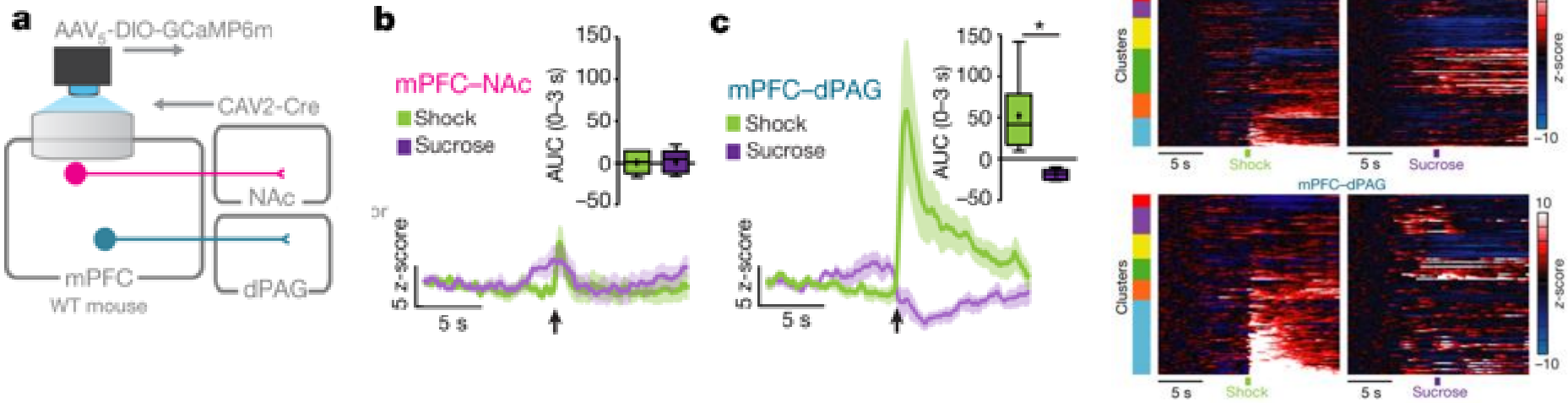

Dopamine probably modulates the SNR of incoming sensory information

- To test whether dopamine had different effects on the intrinsic excitability of these populations:
  - Whole-cell patch-clamp recordings in acute slice preparations of the mPFC containing VTADA–mPFC terminals expressing ChR2 and retrogradely labelled mPFC–dPAG or mPFC–NAc neurons.

- Delivery of current steps to evoke intermediate levels of neural firing that were paired with photostimulation of VTADA–mPFC neurons on interleaved sweeps.

- Photostimulation of VTADA–mPFC neurons reduced the number of spikes per step for mPFC–NAc neurons, but did not detectably alter the excitability of mPFC–dPAG neurons.

- Dopamine-mediated suppression of mPFC–NAc neurons was blocked by the D2-type dopamine receptor antagonist raclopride.

- Since dopamine did not modulate mPFC–dPAG neurons ex vivo and this population did not robustly express dopamine receptors, the authors considered the possibility that dopamine modulates the SNR of incoming sensory information—a function that is only revealed when such inputs are intact.

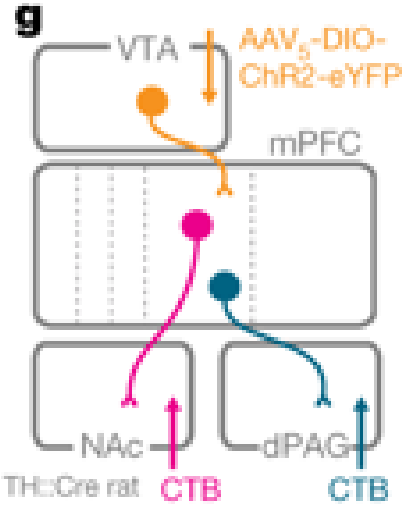

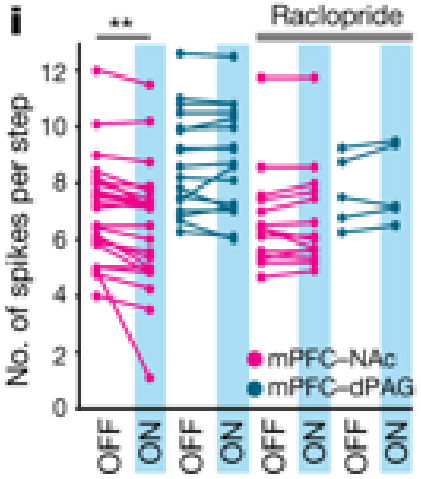

Using inscopix nVoke to confirm the contribution of dopamine released from the VTADA terminals to the modulation of mPFC-dPAG activity

- Simultaneously recording of calcium dynamics in mPFC–dPAG neurons while stimulating VTADA terminals in vivo.

- Expression of the fluorescent calcium sensor GCaMP6m was targeted to mPFC–dPAG neurons, and dopamine neurons were transduced with the depolarizing red-shifted opsin Chrimson29 or mCherry using a dopamine transporter (DAT)::Cre mouse.

- Consistent with the model in which dopamine increases the SNR of mPFC–dPAG activity, VTADA–mPFC stimulation decreased calcium event frequency and increased event amplitude.

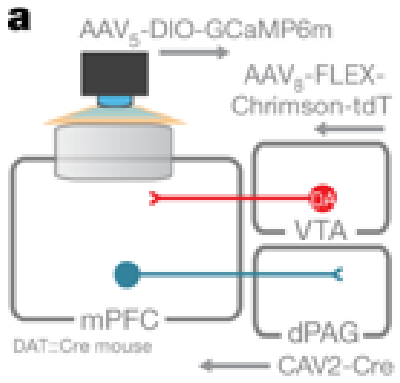

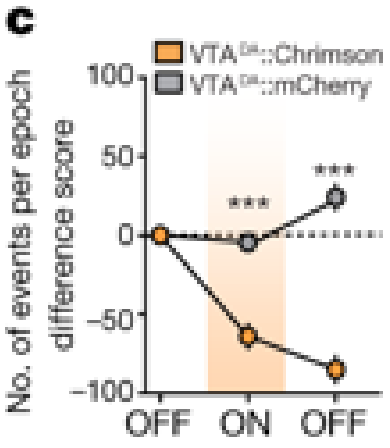

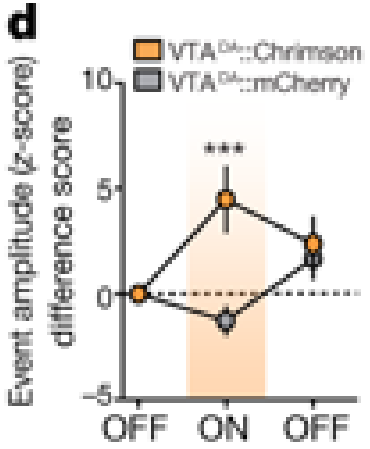

Conclusions

- In vivo microendoscopic imaging has enabled significant advances in the past 5 years in the field of systems neuroscience.

- Further validation is required for the combination of calcium imaging with photoexcitation through optogenetics

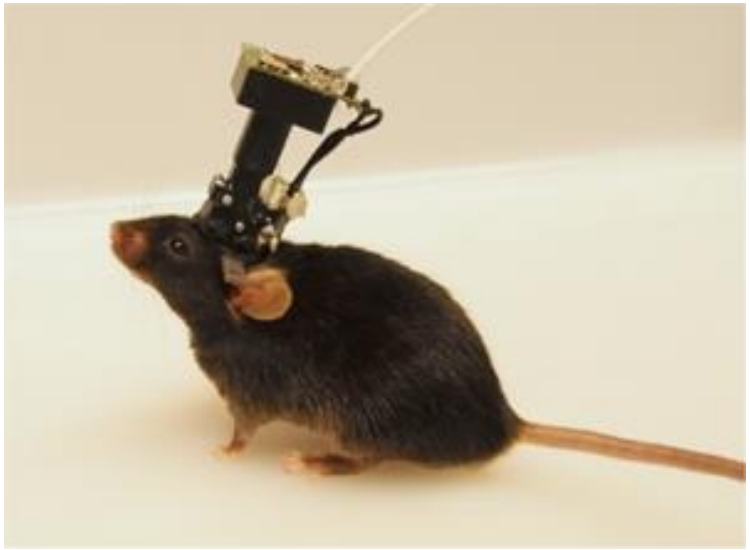

Eisenstein, 2018 Nat Meth